Co-Gasification of Woody Biomass and Sewage Sludge in a Fixed-Bed Downdraft Gasifier

Zhehan Ong
Dept. of Chemical and Biomolecular Engineering, National University of Singapore, Singapore 117585, Singapore

Yongpan Cheng and Thawatchai Maneerung
NUS Environmental Research Institute, National University of Singapore, Singapore 138602, Singapore

Zhiyi Yao, Yen Wah Tong, and Chi-Hwa Wang
Dept. of Chemical and Biomolecular Engineering, National University of Singapore, Singapore 117585, Singapore

NUS Environmental Research Institute, National University of Singapore, Singapore 138602, Singapore

Yanjun Dai
School of Mechanical Engineering, Shanghai Jiaotong University, Shanghai 200240, China

DOI 10.1002/aic.14836
Published online April 20, 2015 in Wiley Online Library (wileyonlinelibrary.com)

Experimental and numerical studies of cogasification of woody biomass and sewage sludge have been carried out. The gasification experiments were performed in a fixed-bed downdraft gasifier and the experimental results show that 20 wt % dried sewage sludge in the feedstock was effectively gasified to generate producer gas comprising over 30 vol % of syngas with an average lower heating value of 4.5 MJ/Nm^3. Further increasing sewage sludge content to 33 wt % leads to the blockage of gasifier, which is resulted from the formation of agglomerated ash. The numerical models were then developed to simulate the reactions taking place in four different zones of the gasifier (i.e., drying, pyrolysis, combustion, and reduction zones) and to predict the producer gas composition and cold gas efficiency. The deviation between the numerical and experimental results obtained was lower than 10%. © 2015 American Institute of Chemical Engineers
AIChE J, 61: 2508–2521, 2015
Keywords: waste-to-energy, biomass gasification, sewage sludge, downdraft gasifier, kinetic modeling

Introduction

Global energy consumption has been increasing steadily and it has become one of the critical challenges throughout the world. Currently, most of the energy consumed comes from fossil-based fuels such as petroleum, coal, and natural gases. On one hand, the limited and nonrenewable fossil-based fuels have been rapidly consumed and will be depleted in the near future; on the other hand, energy generation from fossil-based fuels is also the major source for CO_2 emission[1] (about 41%) which is the major greenhouse gas contributing to global warming. To resolve the energy shortage and relieve global warming, biomass can be considered a potential new and clean energy source. Biomass is a CO_2 neutral and environmentally friendly energy source, as it is formed by the plant photosynthesis process, which absorbs CO_2 from the atmosphere. So far, there are many studies on the conversion of biomass into energy via various processes.[2–9]

Sewage sludge is the solid waste generated from the treatment plant of municipal and industrial wastewaters, and it usually contains organic matter, nutrients, and metals.[10,11] As urbanization and economic development increases dramatically worldwide over the past two centuries, the production of sewage sludge has been dramatically increased. The disposal management of sewage sludge is also difficult due to the presence of toxic and harmful substances such as heavy metals, bacteria, viruses, nonbiodegradable organic compounds, dioxins, and so on.[12] Improper management of sewage sludge can cause serious air, soil, and water pollutions.

To utilize biomass and sewage sludge and reduce their pollution for environment, gasification provides an attractive process, in which biomass and/or sewage sludge is converted to fuels or synthesis gas (a mixture of carbon monoxide and hydrogen). With proper cleaning of the fuels and gases produced, they can be directly used in electricity and heat production devices, such as internal combustion engines, gas turbines, and fuel cells.[13,14] Recently, cogasification of sewage sludge with biomass has attracted much more attention.[15–17] This is because the sewage sludge usually has high moisture and ash contents, and low heating value, hence the gasification of pure sewage sludge results in the low energy production efficiency. Pinto et al.[18] found that the addition of sewage sludge during coal gasification increases the calorific

Additional Supporting Information may be found in the online version of this article.

Correspondence concerning this article should be addressed to C. H. Wang at chewch@nus.edu.sg.

value of the producer gas and fuel conversion. Moreover, they also studied cogasification of sewage sludge with biomass and it was found that the addition of biomass not only increases the production of syngas, but also minimizes the formation of undesirable gases usually generated from sludge gasification.[19]

Although there are many studies on the cogasification of sludge and biomass, there is limited knowledge available in literature relating to the cogasification of sewage sludge and woody biomass in a downdraft gasifier. Additionally, the sewage sludge composition varies between different sources, which significantly affect gasification performance as well as quality of the producer gas. In this study, cogasification of woody biomass and sewage sludge was experimentally investigated using a fixed-bed downdraft gasifier. The temperature distribution in the gasifier, producer gas compositions, and heating values during cogasification of sewage sludge and woody biomass were investigated using different air flow rates and feedstock compositions.

As gasification experiments are usually quite expensive and time-consuming, numerical simulation provides an efficient alternative way to carry out such studies for providing guidance to design the gasifier and optimize the experiments. The gasification has been modeled through either equilibrium, kinetic, or neural network modeling.[20] However, due to its complexity, most of such work was focused on modeling just one or two stages of the process. In Sharma's application[21] of this approach, he specified a full equilibrium model of global reduction reactions in a downdraft gasifier to predict the composition of various gas species, unconverted char, and reaction temperature, yielding reasonable results. Ningbo and Aimin[22] chose to adopt kinetic equations which are only suitable for the pyrolysis and reduction zones, whereas the combustion zone was ignored to simplify the reaction kinetics. Similarly, Giltrap et al.[23] did not consider the pyrolysis and cracking reactions in their model due to the complexities of dealing with numerous possible pyrolysis products. Instead, they employed the kinetic parameters developed by Wang and Kinoshita[24] to simulate gas composition and temperature in the char reduction zone. Babu and Sheth[25] further improved the model by incorporating variable char reactivity factors (CRFs) in place of constant CRF assumed by Giltrap et al.,[23] resulting in the better agreement with experimental data. In this study, the numerical models for drying, pyrolysis, combustion, and reduction zones were built up individually, and then the numerical models for those four zones were combined into one single model and used to reflect the overall performance of gasifier. After validation with experimental data, the characteristics of gasifier [e.g., variations in each reaction zone of the gasifier, producer gas composition, and cold gas efficiency (CGE)] under different composition of sewage sludge and biomass can be easily obtained through the developed numerical simulation.

Experimental Setup and Feedstock Characterization

Figure 1 shows the schematic diagram with brief geometry information of the fixed-bed downdraft gasifier (All Power Labs, Berkeley, CA) employed in this study. The sewage sludge was collected from the wastewater treatment plant under Singapore's Public Utilities Board. Due to sewage sludge has high moisture content, therefore, it must be dried (maximum moisture content of 30%) before gasification. Conversely, wood chips (average dimension: 35 mm length; 10 mm width; and 2.5 mm thickness) were used as another feedstock. The sewage

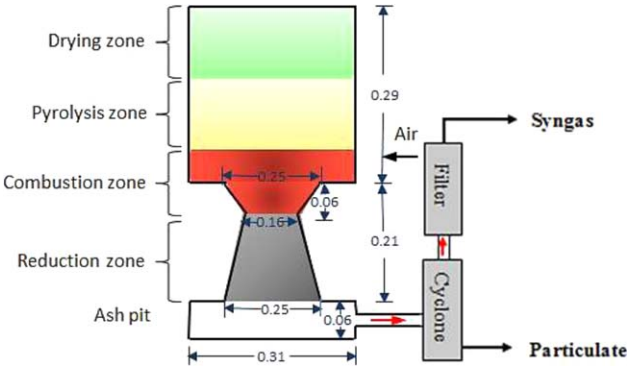

Figure 1. Schematic diagram of fixed bed downdraft gasifier.

[Color figure can be viewed in the online issue, which is available at wileyonlinelibrary.com.]

sludge and wood chips with different mixing ratios were fed into the gasifier from the top. After that, a mixture of feedstock was moved down through four different reaction zones (i.e., drying, pyrolysis, combustion, and reduction zones) inside the gasifier. The controlled amount of air (as an oxidizing agent) was then introduced into the combustion zone through a nozzle with the check valve. The producer gas was finally produced and flowed out from the reaction zone of gasifier to the cyclone and filter to remove the particulates and purify the producer gas, respectively. After that, the producer gas was introduced to internal combustion engine to generate electricity or flare stake for combustion. In the meanwhile, the flow rate and composition of producer gas were also analyzed.

Proximate analysis was conducted through thermogravimetric analysis (TGA) by using Shimadzu DTG-60AH thermal analyzer. The analysis was performed by increasing the temperature from 25 to 800°C with a heating rate of 20°C/min under two different atmospheres (i.e., N_2 and air). Ash content was then calculated from the weight of solid residue remained after the analysis. Conversely, fixed carbon content was calculated from the weight difference of solid residues remained after the analysis under two different atmospheres, that is, N_2 and air. Volatile content was then calculated from the total weight after subtracting weight of moisture, fixed carbon, and ash.

Ultimate analysis was conducted through elemental analyzer (Elementar Vario Micro Cube), providing the contents of carbon (C), hydrogen (H), oxygen (O), nitrogen (N), and sulfur (S) in the dried sewage sludge and wood chips. After that, the higher heating values (HHVs) of the feedstock can be calculated using the following equation[26]

$$\mathrm{HHV} = 0.349(M_C) + 1.178(M_H) + 0.101(M_S) - 0.103(M_O) - 0.015(M_N) - 0.021(M_A) \quad (1)$$

where M_C, M_H, M_O, M_S, M_N, and M_A are the mass fractions of carbon, hydrogen, oxygen, sulfur, nitrogen, and ash, respectively.

Numerical model

After the feedstock was fed into the gasifier, it passed through four different zones (i.e., drying, pyrolysis, combustion, and reduction zones) from the top to the bottom of gasifier. The overall reaction schematic for those four zones is shown in Figure 2 and the numerical model of each zone was built up according to their characteristics.

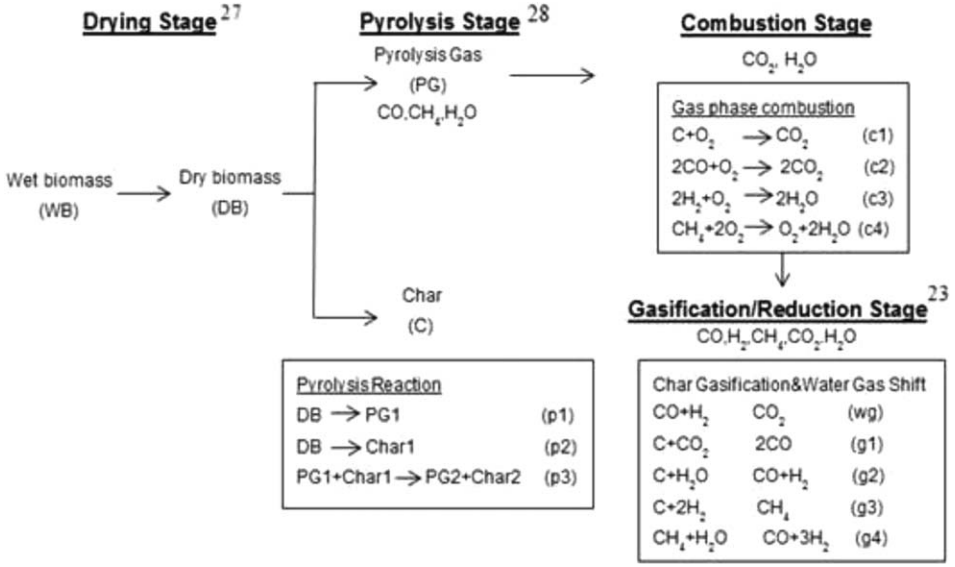

Figure 2. Reaction schematic for biomass gasification.

Drying Zone. Numerical model in the drying zone was built to determine the release rate of moisture after absorbing heat. The developed model was adapted from Besma et al.[27] by incorporating the Eqs. 2–4. Conversely, the remaining moisture in the feedstock that came out from the drying zone will contribute to the steam produced during the pyrolysis process

$$Q_{\text{ext}}=4\pi^2\left(h_T(T_\infty-T_P)+\sigma\varepsilon(T_{\text{react}}^4-T_P^4)\right) \tag{2}$$

$$\frac{dH_{\text{p}}}{dt}=Q_{\text{ext}}-Q_{\text{dry}} \tag{3}$$

where $H_{\text{p}}=(m_{\text{w}}C_{\text{pw}}^{\text{liq}}+m_{\text{s}}C_{\text{psl}})(T_{\text{p}}-T_{\text{ref}})$

$$\rho_{\text{w}}^{\text{vap}}=a_{\text{w}}\rho_{\text{w}}^{\text{sat}} \tag{4}$$

where Q_{ext} is the heat-transfer rate between the particle and its surrounding atmosphere. r is the feedstock particle radius. h_T is the convection heat-transfer coefficient. T_∞ ,, T_{p}, and T_{react} are the temperatures of surroundings, feedstock particle, and reactor, respectively. H_{p} is the particle enthalpy. Q_{ext} is the heat-transfer rate between the particle and its surrounding atmosphere. Q_{dry} is the heat-transfer rate from the drying process. m_{s} and m_{w} are the mass of water and solid matrix, respectively. C_{psl} and $C_{\text{pw}}^{\text{liq}}$ are the heat capacity of solid matrix and liquid water, respectively. $\rho_{\text{w}}^{\text{vap}}$ and a_{W} are the water mass concentration at the surface of the particle in nonsaturated conditions and water activity, respectively. $\rho_{\text{w}}^{\text{sat}}$ is the water mass concentration in saturation. The meaning of variables defined in all equations is shown in Notation.

A summary of the mathematical formulation used to describe the water mass flux during drying is provided in Table 1. Ultimately, a mass balance was used to derive the evolution of water over time

$$\frac{dm_{\text{w}}}{dt}=-F_{m,\text{w}}^{\text{free},T_{\text{p}}}-F_{m,\text{w}}^{\text{bound},T_{\text{p}}}-F_{m,\text{w}}^{\text{free},T_{\text{evap}}}-F_{m,\text{w}}^{\text{bound},T_{\text{evap}}} \tag{5}$$

where $F_{m,w}^{\text{free},T}$ and $F_{m,w}^{\text{bound},T}$ are the mass flow rates of free and bound water extracted from the particle at temperature T_{p} or T_{evap}, respectively.

Pyrolysis Zone. In pyrolysis zone, the dried feedstock was broken down to char and pyrolysis gases (Reaction p1 and p2) with two different reaction orders, as shown in Figure 2. After that, the pyrolysis gases were further reacted with char to produce new types of volatiles, gases, and char (Reaction p3).[28] The reaction rates of those three reactions (r_{p1}, r_{p2}, and r_{p3}) are shown in Table 2. The transient variations of different pyrolysis products were calculated from the following equations[22]

$$\text{Biomass}\quad \frac{dC_{\text{B}}}{dt}=-r_{\text{p1}}-r_{\text{p2}} \tag{6}$$

$$\text{Pyrolysis Gas 1}\quad \frac{dC_{\text{PG1}}}{dt}=r_{\text{p1}}-r_{\text{p3}} \tag{7}$$

$$\text{Char 1}\quad \frac{dC_{\text{C1}}}{dt}=r_{\text{p2}}-r_{\text{p3}} \tag{8}$$

$$\text{Char 2}\quad \frac{dC_{\text{C2}}}{dt}=r_{\text{p3}} \tag{9}$$

$$\text{Pyrolysis Gas 2}\quad \frac{dC_{\text{PG2}}}{dt}=r_{\text{p3}} \tag{10}$$

The pyrolysis gases produced from the pyrolysis zone were hypothesized by Giltrap et al.[23] to be a mixture of CO, CH_4, and H_2O. The atomic balance was used to determine their compositions. After the pyrolysis zone, those pyrolysis gases were then flowed into the combustion zone.

Combustion Zone. In combustion zone, products from the pyrolysis zone were fully oxidized to produce CO_2 and H_2O as well as heat. The heterogeneous and homogeneous reactions which take place inside the combustion zone can be expressed as follows

Table 1. Governing Equations for Drying Process

	Free Water	Bound Water
$T_{\text{p}}<T_{\text{evap}}$	$F_{m,\text{w}}^{\text{free},T\text{p}}=4\pi r^2k_m(\rho_{\text{w}}^{\text{sat}}-\rho_{\text{w}}^{\infty})$	$F_{m,\text{w}}^{\text{bound},T\text{p}}=4\pi r^2k_m(\rho_{\text{w}}^{\text{vap}}-\rho_{\text{w}}^{\infty})$
$T_{\text{p}}=T_{\text{evap}}$	$F_{m,\text{w}}^{\text{free},T_{\text{evap}}}=\frac{Q^{\text{ext}}+Q^{\text{react}}}{\Delta H_{\text{w}}^{\text{vap}}}$	$F_{m,\text{w}}^{\text{bound},T_{\text{evap}}}=\frac{Q^{\text{ext}}+Q^{\text{react}}}{\Delta H_{\text{w}}^{\text{vap}}+\Delta H_{\text{w}}^{\text{des}}}$

k_m is the mass-transfer coefficient, ρ_{w}^{∞} is the water vapor density in surroundings, ΔH_m^{vap} and ΔH_m^{des} are the enthalpy changes of water vaporization and desorption, respectively.

Table 2. Reaction Rates of Individual Pyrolysis Components[28]

R_{xn}	Reaction Rates	Reaction Constants
p1	$r_{p1} = A_{p1} e^{\left(\frac{D_1}{T}+\frac{L_1}{T^2}\right)} C_{DB}^{n1}$	$A_{p1} = 9.973 \times 10^{-5}$ (s^{-1}) $D_1 = 17{,}254.4$ (K) $L_1 = -9{,}061{,}227$ (K^2)
p2	$r_{p2} = A_{p2} e^{\left(\frac{D_2}{T}+\frac{L_2}{T^2}\right)} C_{DB}^{n1}$	$A_{p1} = 1.068 \times 10^{-3}$ (s^{-1}) $D_1 = 10{,}224.4$ (K) $L_1 = -6{,}123{,}081$ (K^2)
p3	$r_{p3} = A_{p3} e^{\left(-\frac{E_3}{RT}\right)} C_{PG1}^{n2} C_{char1}^{n3}$	$A_{p3} = 5.7 \times 10^{-5}$ (s^{-1}) $E_3 = 81{,}000$ (J/mol)

$$C + O_2 \rightarrow CO_2 \quad (c1)$$

$$2CO + O_2 \rightarrow 2CO_2 \quad (c2)$$

$$2H_2 + O_2 \rightarrow 2H_2O \quad (c3)$$

$$CH_4 + 2O_2 \rightarrow CO_2 + 2H_2O \quad (c4)$$

Due to the heterogeneous nature of reaction (c1), it was assumed to have similar manner to the char gasification reaction.[23] As such, this reaction rate still consisted of Arrhenius type temperature dependence, but was also proportional to the actual reactant to product ratio and the corresponding equilibrium ratio.[22] The combustion reactions (c2–c4) were assumed to adopt Arrhenius type dependence on temperature and gaseous compound concentrations. Table 3 presents the reaction rate equations and reaction rate constants of those combustion reactions (c1–c4).[29–31] To determine the final concentrations of the combustion reactants and products, a transient evolution of the respective compounds were derived from the following differential equations

$$O_2 \quad \frac{dO_2}{dt} = -r_{c2} - r_{c3} - 2r_{c4} \quad (11)$$

$$CO \quad \frac{dCO}{dt} = -2r_{c2} \quad (12)$$

$$CH_4 \quad \frac{dCH_4}{dt} = -r_{c4} \quad (13)$$

$$H_2O \quad \frac{dH_2O}{dt} = 2r_{c3} + 2r_{c4} \quad (14)$$

$$H_2 \quad \frac{dH_2}{dt} = -2r_{c3} \quad (15)$$

$$CO_2 \quad \frac{dCO_2}{dt} = 2r_{c2} + 2r_{c4} \quad (16)$$

Reduction Zone. In the reduction zone (the last zone of the gasifier), products from the combustion zone are converted into synthesis gas (a mixture of CO and H_2) and other gases such as CO_2 and CH_4. The reactions which take place inside the reduction zone can be summarized as follows[23]

$$C + CO_2 \leftrightarrow 2CO \quad (g1)$$

$$C + H_2O \leftrightarrow CO + H_2 \quad (g2)$$

$$C + H_2 \leftrightarrow CH_4 \quad (g3)$$

$$CH_4 + H_2O \leftrightarrow CO + H_2 \quad (g4)$$

$$CO + H_2O \leftrightarrow CO_2 + H_2 \quad (g5)$$

The first three reactions (g1–g3) are highly endothermic reduction reactions of char (C) with three different gases, that is, CO_2, H_2O, and H_2, respectively. The fourth reaction (g4) is the reforming reaction CH_4 with steam, producing a mixture of CO and H_2 gases. The final reaction (g5) considered in this model is the water-gas shift reaction.

Table 3. Reaction Rates and Profiles of Individual Combustion Components[29–31]

R_{xn}	Reaction Rates	Reaction Constants
c1	$r_{c1} = A_{c1} e^{\left(-\frac{E_{c1}}{RT}\right)} (P_{CO} - \frac{P_{CO_2}}{K_{c1}})$	$A_{c1} = 5.67 \times 10^9$ ($mol/m^3/s$) $E_{c1} = 160$ (kJ/mol)
c2	$r_{c2} = A_{c2} e^{\left(-\frac{E_{c2}}{T}\right)} C_{CO} C_{O_2}^{0.25} C_{H_2O}^{0.5}$	$A_{c2} = 3.98 \times 10^{14}$ $((m^3/mol)^{-0.75}/s)$ $E_{c2} = 20{,}119$ (K)
c3	$r_{c3} = A_{c3} e^{\left(-\frac{E_{c3}}{T}\right)} C_{H_2} C_{O_2}$	$A_{c3} = 2.19 \times 10^{12}$ $((m^3/mol)^{-1}/s)$ $E_{c3} = 13{,}127$ (K)
c4	$r_{c4} = A_{c4} e^{\left(-\frac{E_{c4}}{T}\right)} C_{CH_4}^{0.7} C_{O_2}^{0.8}$	$A_{c4} = 1.58 \times 10^{13}$ $((m^3/mol)^{-0.5}/s)$ $E_{c4} = 24{,}343$ (K)

Due to the equilibrium nature of those reactions, equilibrium constants are required to calculate the reaction rates. The equilibrium constants of those reactions were obtained from NASA coefficient fits on JANAF tables.[34] The Arrhenius type temperature dependence was assumed and coupled with a proportional dependence between the reactant-to-product ratio and corresponding equilibrium constant. Conversely, the frequency factor (A_i) incorporated with the CRF was used to represent the relative reactivity of char. Table 4 shows the reaction rates and the corresponding values of their reaction constants.[24] The net formation rate for each gaseous species can be then derived from the reaction rates and further used to calculate the molar concentrations of each gaseous species, which can be summarized as follows

$$CO \quad R_{CO} = 2r_{g1} + r_{g2} + r_{g4} \quad (17)$$

$$CH_4 \quad R_{CH4} = r_{g3} - r_{g4} \quad (18)$$

$$H_2O \quad R_{H2O} = r_{g2} - r_{g4} \quad (19)$$

$$H_2 \quad R_{H2} = r_{g2} - 2r_{g3} + 3r_{g4} \quad (20)$$

$$CO_2 \quad R_{CO2} = -r_{g3} \quad (21)$$

Based on the net formation rate of each species, the one-dimensional spatial derivative of each compound can be derived,[23] as shown in Eq. 22

Table 4. Reduction Stage Reaction Rates[24]

R_{xn}	Reaction Rates	Reaction Constants
g1	$r_{g1} = A_{g1} e^{\left(-\frac{E_{g1}}{RT}\right)} (P_{CO_2} - \frac{P_{CO}^2}{K_1})$	$A_{g1} = 3.616 \times 10^4$ (s^{-1}) $E_{g1} = 77.39$ (kJ/mol)
g2	$r_{g2} = A_{g2} e^{\left(-\frac{E_{g2}}{RT}\right)} (P_{H_2O} - \frac{P_{CO} P_{H_2}}{K_3})$	$A_{g2} = 1.517 \times 10^7$ (s^{-1}) $E_{g2} = 121.62$ (kJ/mol)
g3	$r_{g3} = A_{g3} e^{\left(-\frac{E_{g3}}{RT}\right)} (P_{H_2}^2 - \frac{P_{CH_4}}{K_2})$	$A_{g3} = 4.189$ (s^{-1}) $E_{g3} = 19.21$ (kJ/mol)
g4	$r_{g4} = A_{g4} e^{\left(-\frac{E_{g4}}{RT}\right)} (P_{CH_4} P_{H_2O} - \frac{P_{CO} P_{H_2}^3}{K_4})$	$A_{g4} = 73.01$ (s^{-1}) $E_{g4} = 36.15$ (kJ/mol)
g5	$r_{wg} = A_{wg} e^{\left(-\frac{E_{wg}}{RT}\right)} (P_{CO_2} P_{H_2} - \frac{P_{CO} P_{H_2O}}{K_{wg}})$	$A_{wg} = 2.824 \times 10^1$ (s_{-1}) $E_{wg} = 32.84$ (kJ/mol)

$$(n_x A v)|_z = (n_x A v)|_{z+\Delta z} + R_x A \Delta z \quad (22)$$

where n_x is the molar density of species x, n is the summation of n_x of all species. A and z refer to the area of gasifier and axial distance in the gasifier, respectively. v is the superficial gas velocity. R_x is a formation rate of species x.

Assuming $\Delta z \rightarrow 0$ and taking the first derivative, the differential equation characterizing the molar balances of each gaseous species can be written as follows ($x = CO$, CH_4, H_2O, H_2, and CO_2)

$$\frac{dn_x}{dz} = \frac{1}{v}\left(-R_x - n_x \frac{dv}{dz}\right) \quad (23)$$

Similarly, the derivation of the energy balance was also based on the same theory that any change in energy flow rate over a small distance (Δz) must be equal to the net rate of energy produced. Procuring the necessary values of C_p and $H(T)$ detailed earlier, the energy balance can be written as follows

$$\left[v\left(\sum_x n_x c_x T\right)\right]\Bigg|_{z+\Delta z} - \left[v\left(\sum_x n_x c_x T\right)\right]\Bigg|_z = \sum_x r_i \Delta H_i \Delta z - \Delta(PAv) \quad (24)$$

where ΔH_i is the reaction enthalpy of the species i. P is the total pressure of all gaseous species. c_x is the molar heat capacity.

After dividing throughout by $A\Delta z$ and taking $\Delta z \rightarrow 0$, the final energy balance equation of the reduction process can be written as follows

$$\frac{dT}{dz} = \frac{1}{v\sum_x n_x c_x}\left(\sum_x r_i \Delta H_i - v\frac{dP}{dz} - P\frac{dv}{dz} + \sum_x R_x c_x T\right) \quad (25)$$

Two more equations were applied to complete the system of differential equations: (1) superficial gas velocity and (2) pressure profile. The empirical formula used to find the pressure gradient of a fluid flowing through a bed of solid char particles is shown in Eq. 26[23,25]

$$\frac{dP}{dz} = 1183\left(\rho_{gas}\frac{v^2}{\rho_{air}}\right) + 388.19\, v - 79.896 \quad (26)$$

where ρ_{gas} and ρ_{air} refer to the density of gas and air, respectively. Differentiation of the ideal gas law with respect the z gave Eq. 27

$$\frac{dP}{dz} = \frac{dn}{dz}RT + nR\frac{dT}{dz} \quad (27)$$

The summation of the term $\frac{dn_x}{dz}$ for each gaseous species can result in the spatial variation rate of the total gas mixture, $\frac{dn}{dz}$. This value and the empirical correlation derived for $\frac{dP}{dz}$ were then substituted into Eq. 27. After rearrangement, the term $\frac{dv}{dz}$ can be written as follows

$$\frac{dv}{dz} = \frac{1}{\sum_x n_x c_x + nR}\left[\sum_x \frac{\sum_x n_x c_x \sum_x R_x}{n} - \frac{\sum_x r_i \Delta H_i}{T} - \frac{dP}{dz}\left(\frac{v}{T} + \frac{v\sum_x n_x c_x}{P}\right) + \sum_x R_x c_x\right] \quad (28)$$

Equations 23, 25, 26, and 28 represent the mass and energy balance equations for the entire system. Therefore, a set of nine first-order ordinary differential equations in the reduction zone can be then obtained and the axial profile of the producer gas composition within the reduction zone can be finally developed using those equations.

Based on the governing equations from the drying zone to the reduction zone, the overall process occurring during the biomass and sewage sludge gasification can be simulated. The operating and geometrical parameters of the gasifier as well as the characteristics of feedstock (which are based on the experimental measurement) used as the model inputs are summarized in Table 5.

Table 5. Biomass and Gasifier Characteristics as Model Inputs

Source	Present Study	Present Study
Biomass type	Wood chips	33% Sewage sludge + 67 % Wood chips
Biomass Characteristics		
Density (kg/m^3)	500	440.6
Gasifier Characteristics		
Biomass feed rate (kg/h)	10	10
Air flow rate (L/s)	7	7
Time in drying zone (min)[a]	5	5
Time in pyrolysis zone (min)[b]	10	10
Air temperature (°C)	30	30
Reduction zone length (m)	0.25	0.25

[a]Calculated timing given height of drying zone, diameter of drying zone, density of biomass and biomass introduction rate.
[b]Critical time needed for biomass to pyrolyse to 10% of its original mass, which was estimated from schematic given in the studies of Dogru et al.[33]

Results and Discussion

Experimental results

Feedstock Characterization. Table 6 shows the TGA results of wood chips and dried sewage sludge. It was found that the dried sewage sludge has higher ash content and a lower amount of volatile compounds and fixed carbon contents as compared to the wood chip. Moreover, it was also

Table 6. Proximate, Ultimate Analysis, Heating Value of Feed Stocks

Feedstock	Sewage Sludge[a]	Wood Chips
Proximate analysis (dry basis, wt %)		
Moisture	5.8–9.4	8.2–8.5
Volatiles	49.8–51.8	67.8–69.2
Fixed carbon	14.3–15.9	16.2–17.5
Ash	22.8–29.7	6.2–6.3
Ultimate analysis (wt %)		
Carbon	33.5–36.42	43.3–44.2
Hydrogen	4.2–5.4	5.4–6.1
Oxygen	24.1–31.5	41.6–42.5
Nitrogen	4.9–5.5	0.9–2.1
Sulfur	1.5–1.9	0.5–1.0
High heating value (MJ/kg)	14.4–15.0	17.0–18.2
Elemental analysis, ICP (ppm)		
Cd	–	–
Co	<0.10	–
Cr	<0.10	–
Cu	0.9–2.9	<0.10
Fe	6.1–10.8	0.1–0.3
Mn	<0.10	<0.10
Ca	5.2–6.7	3.8–3.6
Pb	<0.10	<0.10
Hg	–	<0.10

[a]Typical sewage sludge examples were collected from Ulu Padan wastewater treatment plant, Singapore.

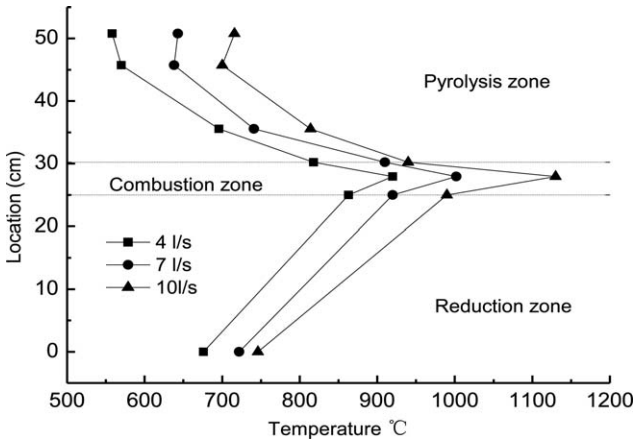

Figure 3. Measured temperature profiles along the height of gasifier under different air flow rates.

found from the ultimate analysis of the dried sewage sludge has lower carbon and hydrogen contents, resulting in the lower heating value (LHV) of sewage sludge as compared to wood chips.

Effect of Air Flow Rate on Temperature Profile in the Gasifier. The temperature profile in the downdraft gasifier as a function of air flow rate from 4.0 to 10.0 L/s was investigated during wood chips gasification. As shown in Figure 3, the temperature distribution inside the gasifier was significantly affected by air flow rate. It was found that the temperature at all locations of the gasifier increased with increasing air flow rate. This is due to the fact that the higher air flow rate promotes the exothermic combustion reactions,[17] releasing more energy, and hence increasing the temperature inside the gasifier. Moreover, it was found that temperatures in the pyrolysis and reduction zones of the gasifier were lower than that in the combustion zone, which is mainly due to the fact that energy are consumed for the pyrolysis and endothermic reduction reactions. The temperature in the pyrolysis zone was in a range of 550–800°C which is high enough for the complete pyrolysis of wood chips and/or sewage sludge to take place. Similar temperature range for the pyrolysis of woody biomass and sewage sludge was also reported in the literature.[34–36] Conversely, the temperature range in the

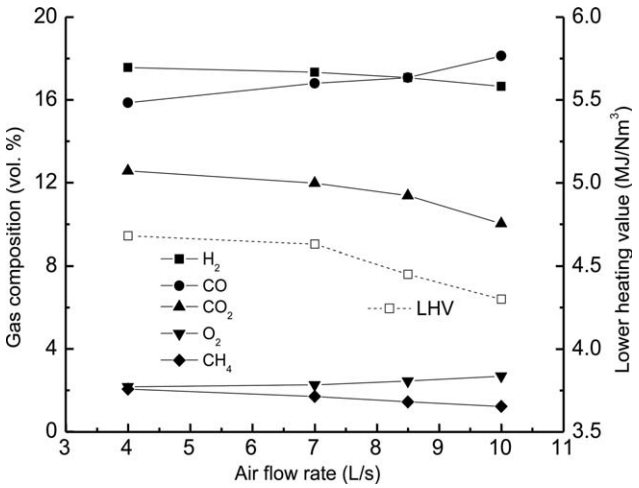

Figure 4. Effect of air flow rate on the producer gas composition and lower heating values.

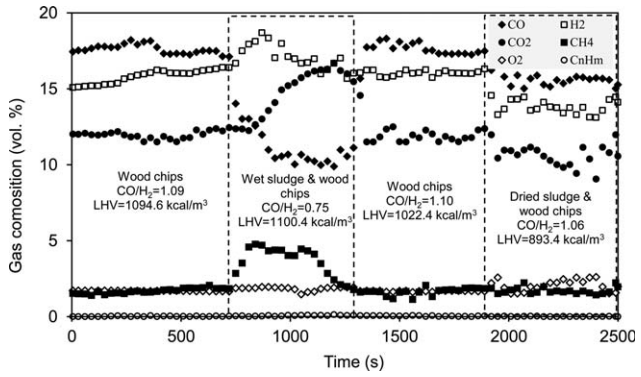

Figure 5. Transient variation of producer gas compositions of wood chips gasification with dried sewage sludge added at 500 s.

reduction zone was found to be 650–950°C which is in the reported range of gasification temperatures (i.e., 550–1000°C).[37]

Effect of Air Flow Rate on Producer Gas Composition. In addition to the effect of air flow rate on the temperature profile, it is also of great interest and importance to investigate the effect of air flow rate on the producer gas composition. Figure 4 shows the producer gas composition and LHV as a function of air flow rate during gasification of wood chips. It was found that the concentration of CO was significantly increased when the air flow rate was increased from 4.0 to 10.0 L/s. It is well-known that char gasification reactions with CO_2 and steam are favored at high temperatures due to the nature of endothermic reaction.[38] Therefore, the increase in temperature with increasing air flow rate significantly promotes the char gasification reactions, and resulting in the increasing of CO concentration in the producer gas. Conversely, it was found that the concentration of H_2 was slightly decreased with increasing air flow rate. This could be explained by the fact that the increase in temperature by raising the air flow rate promotes the reverse water-gas shift reaction, resulting in the decreasing of H_2 and CO_2 concentrations. This result is also in a good agreement with the literature.[39] The significant decrease in H_2 and CH_4 concentrations in the producer gas, which has a higher calorific value as compared to CO, resulted in a decrease of the LHV. This result is consistent with the previous work done by Seggiani et al.[17] who observed the decreasing of LHV when the air flow rate was increased.

Effect of Moisture in Feeding Materials on Producer Gas Composition. To investigate the effect of moisture content in the sewage sludge on the producer gas composition, cogasification of wood chips and two different forms of sewage sludge, that is, wet sewage sludge (as received, ~80 wt % moisture) and dried sewage sludge (after pretreatment, ~9 wt % moisture) were performed. The variation of the producer gas composition obtained is shown in Figure 5. The composition of producer gas was significantly affected by the moisture content in the sewage sludge. It was found that the concentrations of CO_2, CH_4, and H_2 in the producer gas were remarkably increased, whereas the concentration of CO was decreased when 20 wt % of wet sewage sludge and 80 wt % of wood chips was introduced into the gasifier. As a result, the CO/H_2 ratio was decreased from 1.1 to 0.75 after the feeding of 20 wt % wet sewage sludge into the gasifier. This is mainly due to the fact that the steam generated from the wet sewage

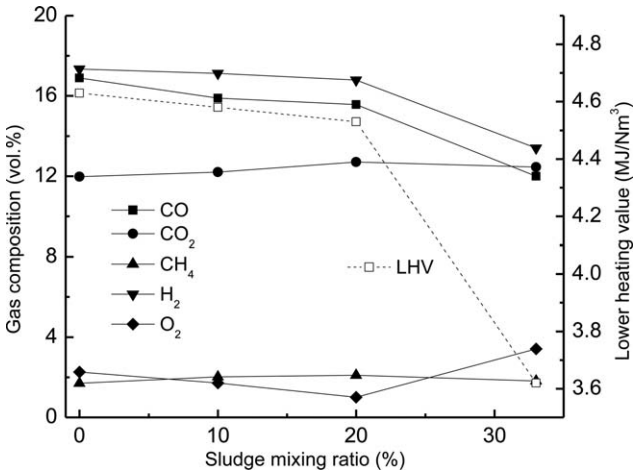

Figure 6. Effect of feed stock composition on (a) producer gas composition and (b) lower heating values during cogasification of sewage sludge and wood chips.

sludge took part in the water-gas shift reaction (g5), converting CO into H_2 and CO_2. Moreover, the temperature inside the gasifier was greatly reduced as heat was consumed to vaporize the moisture in the wet sewage sludge.[32] The decrease in temperature further favors the exothermic water-gas shift reaction, converting more CO. Furthermore, the high concentration of H_2 and low temperature conditions favor the formation of CH_4 via the exothermic reaction (g3), and hence increasing the concentration of CH_4 in the producer gas; this result is in a good agreement with the literature.[40,41]

Conversely, the producer gas composition produced from the cogasification of dried sewage sludge and wood chips is not significantly different from that produced from the gasification of wood chips. However, it can be observed that the amount of the producer gas was slightly decreased during the cogasification of dried sewage sludge and wood chips. This is mainly due to the lower carbon content in the sewage sludge as compared to the wood chips (as shown in Table 6). It should also be noted that the high moisture content (~80 wt %) in the wet sewage sludge could lower the gasification efficiency by consuming energy for the vaporization of moisture and, consequently, changes the producer gas composition. Therefore, dried sewage sludge is preferable for use in cogasification to avoid the aforementioned problems.

Effect of Sewage Sludge to Woody Biomass Ratio on Producer Gas Composition. To determine the optimum amount of sewage sludge in the feedstock, cogasification of four different feedstock compositions (i.e., 0, 10, 20, and 33 wt % dried sewage sludge) was carried out using the air flow rate of 7 L/s and the results obtained are shown in Figure 6. The producer gas volume compositions and LHVs obtained from cogasification of the different feedstock compositions are summarized in Table 7. It was found that the composition of syngas (mixture of CO and H_2) in the producer gas was gradually decreased with increasing sewage sludge content. For example, the gasification of pure wood chips generated 36 vol % of syngas, whereas the cogasification of 20 wt % dried sewage sludge and 80 wt % wood chips generated only 31 vol %. Conversely, the concentration of CO_2 and CH_4 in the producer gas was slightly increased with the increasing of the sewage sludge content. This is due to the lower carbon and hydrogen contents in the sewage sludge as compared to the wood chips which leads to a decrease in overall heating value of the feedstock (as summarized in Table 6). As a consequence, less energy was generated from the combustion reaction when higher sewage sludge content was used, hence resulting in a lower temperature inside the gasifier. For instance, the temperature range in the reduction zone of the gasifier was measured to be approximately 764–940, 746–930, and 720–920°C when the pure wood chips, 10 wt % sewage sludge, and 20 wt % sewage sludge was gasified, respectively. As the char gasification reactions (g1 and g2) are highly endothermic reactions, the decrease in temperature shifts the reaction equilibrium backward to the reactants side, resulting in lower production of CO and H_2, and hence increasing CO_2 concentration. In addition, the decrease in temperature favors the exothermic production of CH_4 (g3), hence resulting in the increasing of CH_4 concentration in the producer gas.

Upon increasing the dried sewage sludge in the feedstock to 33 wt %, the syngas concentration in the producer gas decreased, whereas the O_2 concentration unexpectedly increased. Upon further investigation, it was found that there was a large agglomerated ash (~3 in. cm in diameter) located between the combustion and reduction zones (as shown in Figure 7), blocking the entry of char into the reduction zone, and hence lowering the production of syngas via the char gasification reactions (g1 and g2). Moreover, the blockage also lowered the feeding rate of feed materials entering into the combustion zone, limiting the combustion reaction, and hence resulting in the increase of O_2 composition in the producer gas. Furthermore, it should be noted that the small agglomerated particles (the average particle size ranging from 0.1 to 0.5 in. in diameter) were also found inside the gasifier during cogasification of 10 and 20 wt % dried sewage sludge (as shown in Figures 7b, c, respectively), but the formation of these small agglomerated particles did not cause the blockage of gasifier. Therefore, it

Table 7. Concentration of Gases Produced During Cogasification of Sewage Sludge and Wood Chips

Feed Stocks		Pure Wood Chips	10% Sludge-Mixed Wood Chips	20% Sludge-Mixed Wood Chips[a]	33% Sludge-Mixed Wood Chips
Gas composition (vol %)	CO	17.1	15.9	15.6	12.0
	H_2	17.3	17.1	16.8	13.4
	CH_4	1.7	2.0	2.1	1.8
	CO_2	11.9	12.2	12.7	12.5
	O_2	1.3	1.7	1.0	3.4
	Total	49.1	48.9	48.2	43.1
Lower heating value (MJ/Nm^3)		4.7	4.6	4.5	3.6

[a]Optimum composition of sewage sludge and wood chips for cogasification.

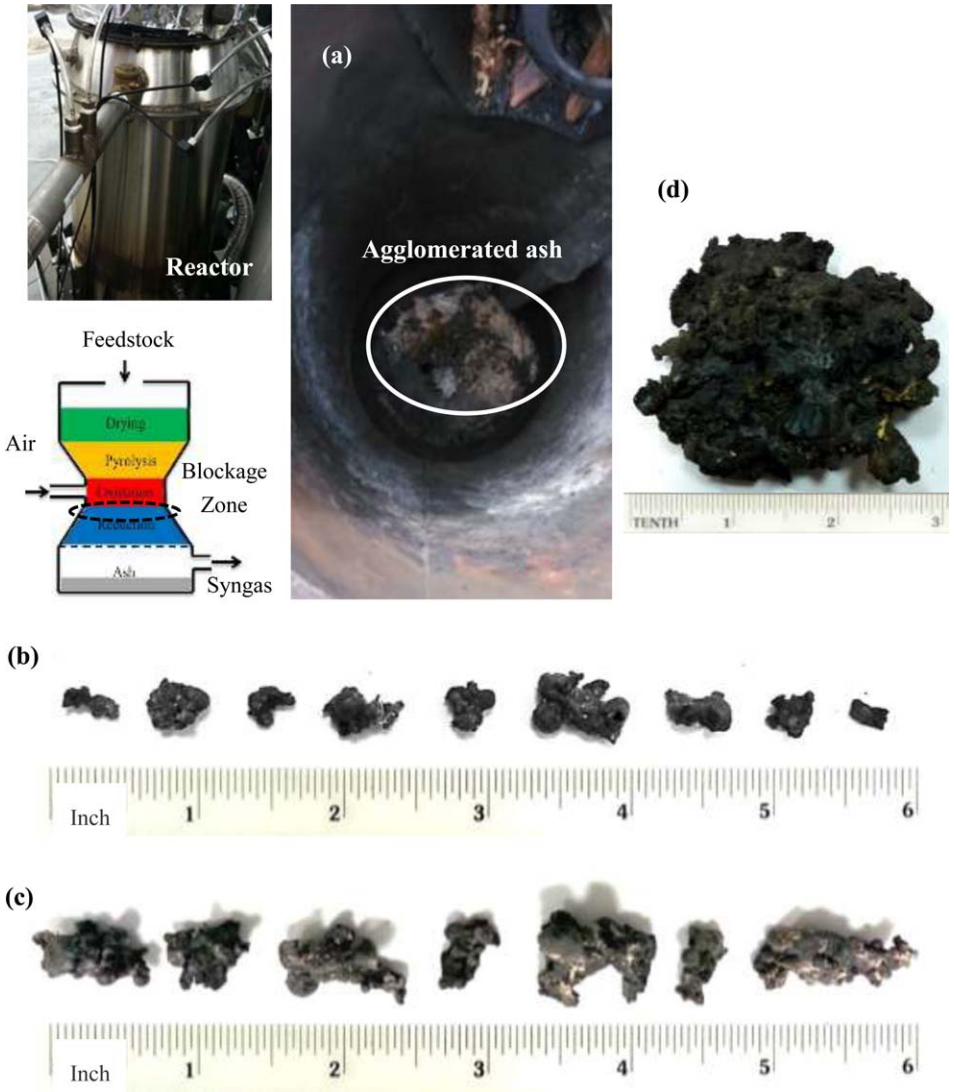

Figure 7. (a) Reactor blockage caused by the agglomeration of ash particles in the reduction zone of gasifier and the agglomerated ash particles found inside gasifier from cogasification of sewage sludge and wood chips at different sewage sludge and wood chips compositions: (b) 10 wt %, (c) 20 wt %, and (d) 33 wt % of the dried sewage sludge, respectively.

[Color figure can be viewed in the online issue, which is available at wileyonlinelibrary.com.]

can be concluded that the optimum content of dried sewage sludge in the feedstock for cogasification in the downdraft fixed-bed gasifier is 20 wt % dried sewage sludge. A comparison of our results with the previous works (as illustrated in Table 8) shows that the performance of gasifier is good in comparison to other systems.[18,42,43]

Blockage of Reactor. As aforementioned, cogasification of 33 wt % dried sewage sludge and 67 wt % wood chips was unsuccessful due to the formation of large agglomerated ash at the initial stage of the reduction zone of the gasifier, blocking the gasifier. Several analyses such as XRD, SEM, and EDX were then used to determine the nature and

Table 8. Comparison of Gasifier Performance with Previous Studies

	Pinto et al.[18,19]	Gai et al.[42]	Kim et al.[43]	This Work	This Work
Type	Fixed-bed	Fixed-bed	Fluidized-bed	Fixed-bed	Fixed-bed
Fuel	Sludge-wood pellets	Corn straw	Wood pellet	Wood chips	Sludge-wood chips[a]
Method	Air	Air	Air	Air	Air
Temperature (°C)	600–1000	700–1100	750–800	700–1000	700–1000
CO	14.2	18.9	16.1	17.1	15.6
H_2	4.3	12.7	16.5	17.3	16.8
CO_2	15.2	13.1	16.4	11.9	12.7
CH_4	2.1	4.0	5.3	1.7	2.1
H_2/CO	0.98	0.70	1.01	1.01	1.07

[a]20% sludge-mixed wood chips (optimum composition).

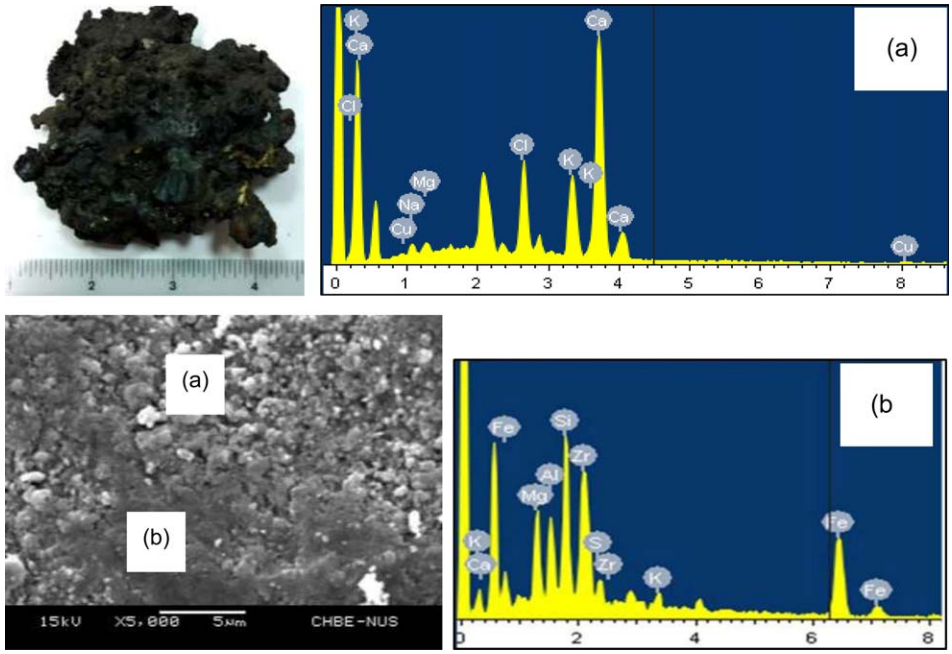

Figure 8. SEM image and EDX analysis of agglomerated ash particle formed during cogasification of 33 wt % sludge and 67 wt % wood chips.

[Color figure can be viewed in the online issue, which is available at wileyonlinelibrary.com.]

chemical composition of the agglomerated ash in order to understand the cause of the agglomeration.

Figure 8 shows the scanning electron microscope (SEM) image and energy-dispersive x-ray spectroscopy (EDX) spectra characterizing the morphology and elemental composition of the agglomerated ash obtained from the cogasification of 33 wt % dried sewage sludge. It was found that the agglomerated ash contains two main elements, calcium (Ca) and iron (Fe), with smaller amount of other elements, which are usually found in the sewage sludge, such as Si, Al, Cl, Cu, and so on. From the inductively-couple plasma spectroscopy (ICP) analysis of wood chips and sewage sludge (as summarized in Table 6), it can be observed that sewage sludge and wood chip contain large amount of Fe and Ca elements, respectively. However, there is no any agglomerated ash formed from the gasification of pure wood chips (as shown in Figure 8a). Therefore, it is reasonable to be concluded that the fusion of Fe with other elements caused the formation of the agglomerated ash during the cogasification of the dried sewage sludge and wood chips. Moreover, mineralization x-ray diffraction (XRD) analysis of agglomerated ash and mechanism for formation of agglomerated ash are presented in Supporting Information.

Mass Balance and Energy Efficiency. Figure 9a shows an overall illustration of total mass balance and energy efficiency of the gasifier at the total flow rate of 7 L/s. Wood chips, which have 18 MJ/kg of HHV, were transported into the reactor with the consumption rate of 10 kg/h. Air was fed into the combustion zone at the flow rate of 7 L/s. Four main reactions, that is, drying, pyrolysis, combustion, and reduction (or gasification) take place inside the gasifier. After all, syngas was finally generated from the reduction zone with the approximated production rate of 7L/s, and its HHV can reach to 5.0 MJ/Nm^3. Moreover, about 2 kg/h of ash was also produced at the bottom of the gasifier.

CGE was then determined to indicate efficiency of the gasifier. The use of this CGE ratio enables the capturing of the key variables that ultimately contributes to efficiency of the gasifier into a single quantifiable value. The CGE is defined as a ratio of energy obtained from the producer gas per kg of biomass to HHV of the biomass consumed,[33] as shown in Eq. 29. From calculation, the CGE of wood chips gasification can reach to 66.9%.

$$CGE = \frac{Dry\ Gas\ HHV\ \left(\frac{MJ}{m^3}\right) \times Syngas\ Prodcction\ Rate\ \left(\frac{m^3}{kg\ biomass}\right)}{Biomass\ HHV\ \left(\frac{MJ}{kg}\right)} \tag{29}$$

Conversely, the total mass balance and energy efficiency of cogasification of wood chips and dried sewage sludge is shown in Figure 9b. It can be seen that the HHV of both feedstock and syngas decreased when 80% of wood chips and 20% of dried sewage sludge was introduced to the gasifier. Moreover, it was also found that the CGE ratio was slightly decreased from 66.9 to 63.2%, indicating that the addition of sewage sludge to the gasifier lower the total energy efficiency of gasifier, as discussed previously.

Numerical results

Model Validation. To validate the numerical model developed, numerical simulations were conducted based on the operating and geometrical parameters (presented in Table 5) and feedstock characterization (presented in Table 6). The

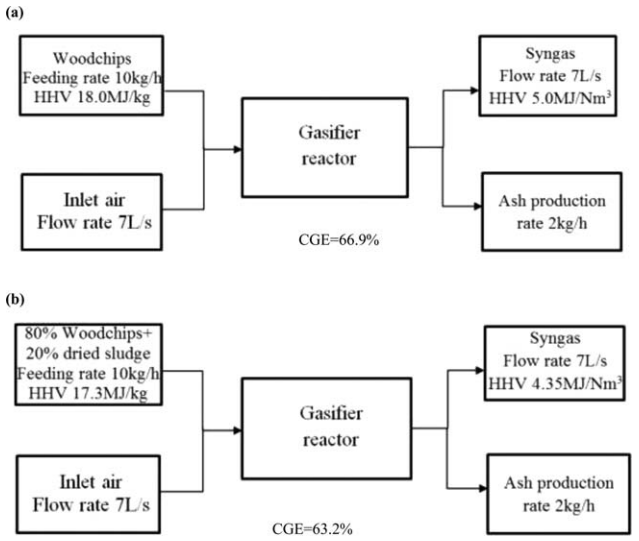

Figure 9. Mass balance and energy efficiency for (a) wood chips gasification and (b) cogasification of wood chips and sewage sludge.

predicted producer gas compositions were then compared with the measured experimental data, as shown in Figure 10. When comparing with wood chips gasification, it was found that the predicted gas composition was in quantitative agreement with

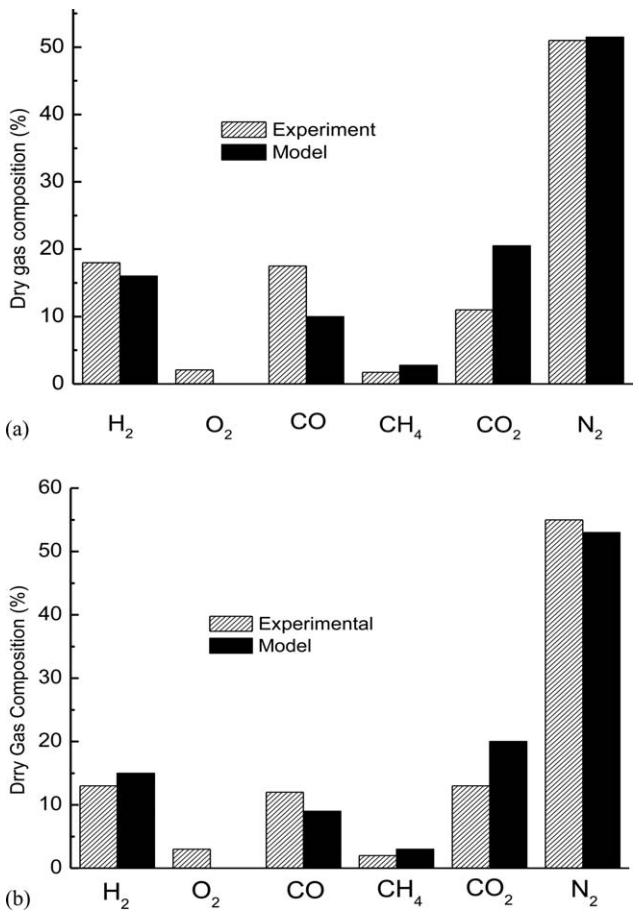

Figure 10. Comparisons of producer gas composition obtained from the gasifier between experimental data and numerical results: (a) wood chips and (b) mixture of 33 wt % dried sewage sludge and 67 wt % wood chips.

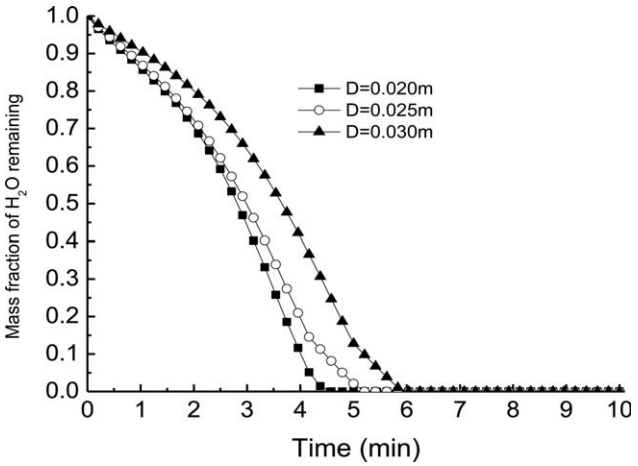

Figure 11. Transient mass fraction of remaining moisture during drying of the feedstock.

the experimental data while the model overpredicted the volume fraction of CO_2 by 8.9% and underpredicted that of CO by 6.63%. In the comparison of cogasification of 33% of sewage sludge and 67% of wood chips, the agreement of the volume fraction of H_2 and CO was quite satisfactory, and the largest deviation came from the volume fraction of CO_2, which was overpredicted by 6.57%.

Drying Process. Figure 11 shows the relative remaining moisture fraction over the initial moisture fraction in the wood chip as a function of time. It was found that the drying rate of feedstock is dependent on the size of feedstock, that is, the larger diameter of feedstock, the slower the drying rate. It should be noted that the initial moisture fraction of wood chips is about 8.35%, as shown in Table 6. According to the height and diameter of drying zone, density and feeding rate of wood chips, the residence time of wood chips in the drying zone is approximately 5 min. After the feed stocks passed through the drying zone, the relative moisture fraction of feed stocks with diameters of 0.02, 0.025, and 0.03 m was decreased to 0, 2, and 12%, respectively. However, it should be noted that the remaining moisture in the

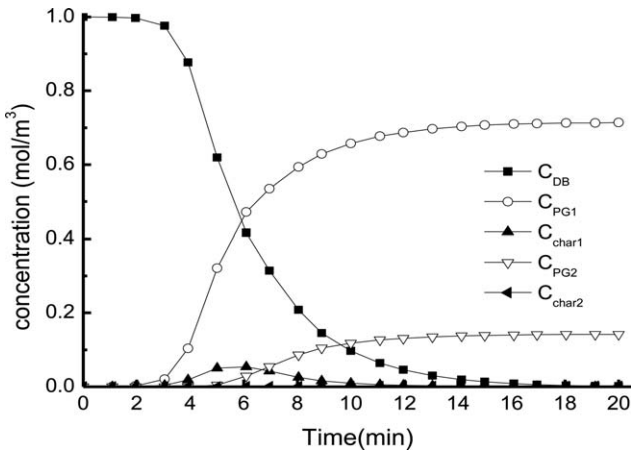

Figure 12. Transient variations of compounds during pyrolysis process.

The symbol C_{DB} refers to the concentration of dry biomass. C_{PG1} and C_{PG2} refer to the concentrations of two types of pyrolysis gases including CO, CH_4, and H_2O of different compositions. C_{char1} and C_{char2} refer to the concentrations of two types of char in the pyrolysis zone.

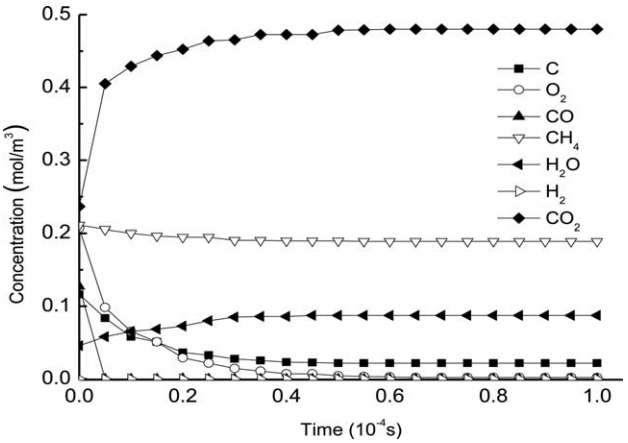

Figure 13. Transient variations of compounds in the combustion process.

feed stocks has an advantage, that is, steam generated from the remaining moisture can be used to produce more hydrogen via the water-gas shift reaction.

Pyrolysis Process. Figure 12 shows the transient variations of various compounds during pyrolysis process. It was found that amount of feedstock was dramatically decreased, while the productions of pyrolysis gases and char were dramatically increased at the initial stage. The fraction of char reached the maximum after 5 min and started to decrease because char was further reacted with the pyrolysis gases. The residence time in the pyrolysis zone was assumed to be approximately 10 min (as shown in Table 6), which is reasonable because the fractions of char and pyrolysis gases almost remained constant after 10 min.

Combustion Process. As can be seen in Figure 13, the combustion (which is a very fast process) took only several microseconds to reach the steady state. As the equivalence ratios were smaller than one, the oxygen in the system was mostly consumed for the combustion process. As a consequence, the oxygen content after the combustion zone almost reached zero, whereas the CO_2 and H_2O contents were increased due to the oxidation of CO, hydrogen, and carbon.

Reduction Process. Figure 14 shows the axial distribution of gas composition in the reduction zone. It can be observed that the volume fractions of CO and H_2 were dramatically increased along the reduction zone, then reached the maximum of 12 and 10%, respectively, at the outlet.

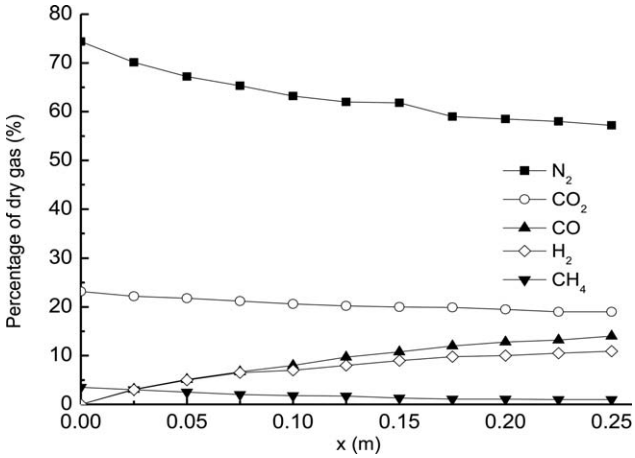

Figure 14. Axial variations of produced gases in the reduction zone.

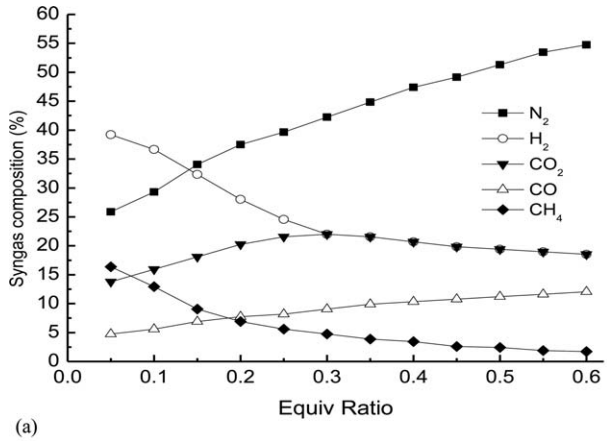

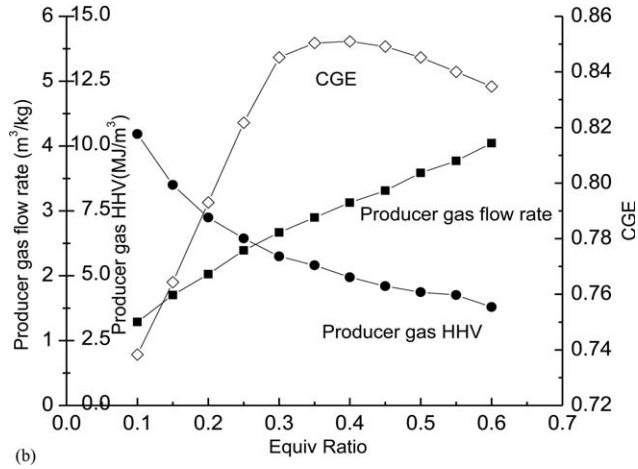

Figure 15. Effect of equivalence ratio on (a) producer gas composition; (b) higher heating values, flow rate, and cold gas efficiency.

Conversely, the volume fraction of CO_2 was gradually decreased from 24% at the inlet to 18% at the outlet.

Effect of Equivalence Ratio on Producer Gases. In this section, the equivalence ratio (φ) and CGE were determined to characterize the energy efficiency of the overall gasification process. The equivalence ratio (φ) which takes the effects of air flow and biomass feed rate into the account can be defined as follows[19]

$$\varphi = \left(\frac{Air\ Flow\ Rate}{Biomass\ Consumption\ Rate}\right) \Big/ \left(\frac{Air\ Flow\ Rate}{Biomass\ Consumption\ Rate}\right)_{\text{Stoichiometric}} \quad (30)$$

As can be seen in Eq. 30, the computation of φ requires the stoichiometric ratio of air flow rate to biomass consumption rate. The equivalence ratio (φ) has great influence on the efficiency of gasification process. As shown in Figure 15a, it was found that when the equivalence ratio increases, the production of CO was greatly increased from 5 to 12%. This is probably due to the fact that more heat was released from the combustion process, which promotes the char gasification reactions, producing more CO gas. As a result, the volume fractions of H_2 and CH_4 were decreased. This result is in good agreement with the literature.[19] As the inert N_2 gas is not contributed to the HHV and its fraction was

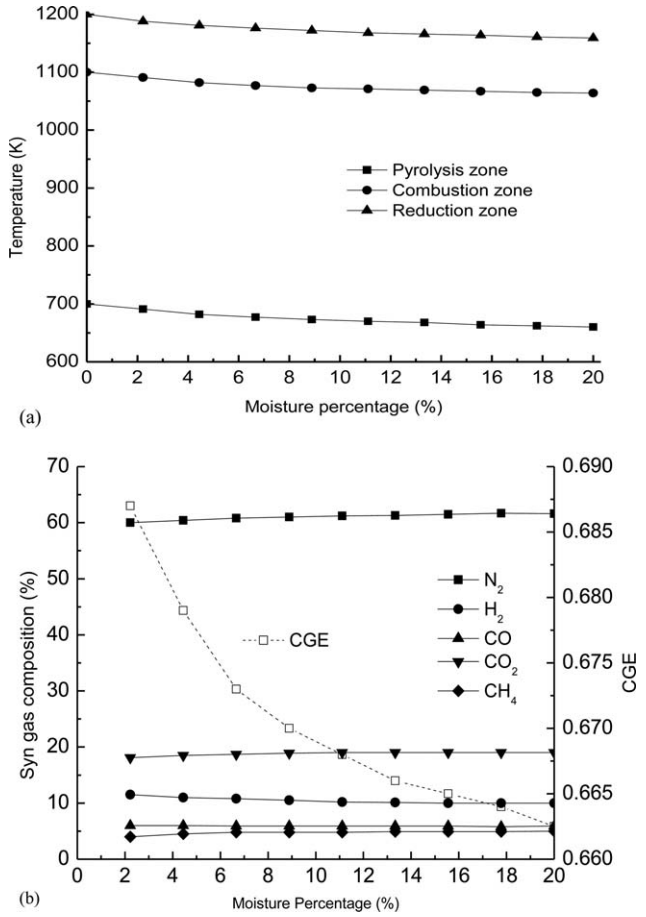

Figure 16. Effects of moisture percentage on (a) temperature profiles of reaction zones; (b) producer gas composition and cold gas efficiency.

dramatically increased from 25 to 55%, the HHV of the producer gas was significantly decreased with the increasing of equivalence ratio. However, with the combination effect of CO, H_2, and CH_4, the producer gas flow rate per unit of biomass were significantly increased, as shown in Figure 15b. This result is also in good agreement with the literature.[45] To evaluate the combined effect of equivalence ratio for syngas flow rate per unit of biomass and HHVs, CGE was plotted against the equivalence ratio. It was found that the optimum equivalence ratio for this down draft gasifier is in a range of 0.35–0.4, providing the maximum value of CGE.

Effect of Moisture Content on Producer Gases. It is known that the increase in moisture content has a detrimental effect on the thermal performance of the gasifier as the evaporation of water is an extremely energy consuming process,[33] higher moisture content requires more energy to evaporate because of the endothermic nature of evaporation. As can be seen in Figure 16a, the temperatures in the pyrolysis, combustion, and reduction zones significantly decreased as the moisture percentage was increased. Figure 16b shows that the concentration of CO slightly decreased, while the concentration of CO_2 increased with the increasing of moisture content. Conversely, there is no significant change in the CH_4 concentration. This is probably because decreasing the temperature promotes water-gas shift reaction (g5). Due to the lower concentration of CO and H_2 with increasing moisture content, the HHVs of producer gas were subsequently decreased, and hence resulting in the lower CGE.

Effect of Sewage Sludge Composition on Producer Gases. . Figure 17 shows the effect of sewage sludge composition in the feedstock on the producer gas. It was found that the producer gas flow rate per unit of biomass decreased when the sewage sludge content was increased from 0 to 30%, this is mainly due to the lower carbon content in sewage sludge as compared to wood chips. This result is consistent with the literature.[17] In the meanwhile, the CGE was also decreased mildly as the content of sewage sludge was increased.

Preliminary economic analysis

Due to the broad scope of this work and small scale of gasification unit used in this study, it is not possible to provide the detailed information and costs-benefits analysis of all possible options. Therefore, the preliminary economic analysis was only made in this work by breaking down the capital cost and potential incomes of gasification process compared with the conventional combustion (or incineration) process which is the main technology employed for the waste disposal in Singapore.

Cost Breakdown. The main technical and cost components of thermal process (incineration and gasification) are typically including:

- Waste reception and sorting
- Incinerator/gasifier with auxiliaries
- Flue gas treatment
- Power generating equipment and auxiliaries
- Bottom/fly ash system
- Air emissions control system
- Building and civils

As compared to the incineration technology, the capital costs for gasification are likely to be higher as the gasification technology is not mature enough to lower the costs. However, it should be taken into account that the reducing atmosphere of gasification process generates lower air emissions as compared to the incineration process, eliminating (or minimizing) the requirement of post-treatment units (such as carbon dioxide capture, nitrogen oxide removal, dioxin removal, and acid gas removal systems) those are highly needed for the incineration plant, and possibly leading to the lower overall cost.

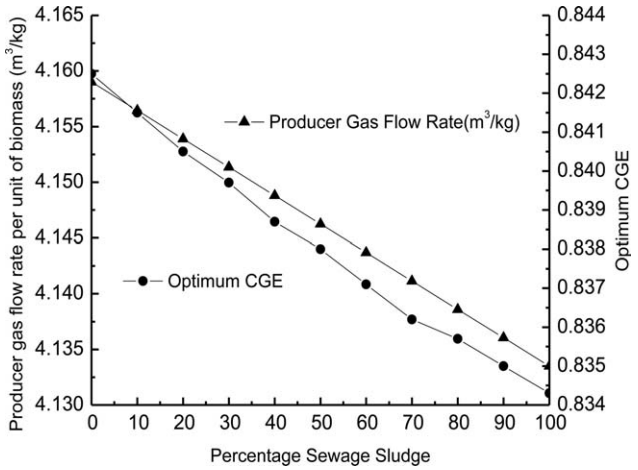

Figure 17. Effects of sewage sludge composition on (a) producer gas composition; (b) cold gas efficiency.

Potential Incomes. For the incineration of sewage sludge operated in Singapore, overall income of the plant comes from the gate fee ($65 is paid to the plant for one ton of sewage sludge processed) and possibly hot steam (that can be generated from the heat released from combustion process) for driving the steam turbines that generate electricity. Conversely, the overall incomes of the gasification plant could come from the gate fee, the syngas that can be directly sold to the chemical production factories or fed to different power generating engines (e.g., steam boilers, reciprocating engines, combined cycle turbines, and fuel cells) to generate electricity,[45] and possibly bottom ash and char (two main by-products from gasification process) which can directly be sold after its verification or further developed into higher value products such as catalytic and absorbent materials.[44]

Although this analysis has not valuated all potential costs and benefits due to the limited information, it is clear that the conversion of solid waste such as biomass and sewage sludge to energy via gasification process has significant environmental advantages and also has the potential to yield net benefits. Moreover, this analysis should be viewed as a screening exercise to find the most promising parameters those are worthy of further, more detailed investigation in the future work.

Conclusions

In this work, both experimental and numerical studies of cogasification of woody biomass and sewage sludge were carried out in order to evaluate the feasibility of using sewage sludge as an alternative source for clean and sustainable energy production. In the experimental section, cogasification of sewage sludge and woody biomass was successfully performed in a fixed-bed downdraft gasifier to produce syngas. A maximum of 20 wt % dried sewage sludge in the feedstock was effectively gasified to generate producer gas comprising over 30 vol % of syngas (a mixture of CO and H_2) with an average LHV of 4.5 MJ/Nm^3. Further increasing the sludge content to 33 wt % leads to the blockage of gasifier; this is mainly due to the formation of agglomerated ash.

The simulation model was then developed by adapting several kinetic models developed in the literature to provide a comprehensive kinetic model for gasification process performed in the fixed-bed downdraft gasifier. The CGE was chosen as the ultimate indicator of gasifier efficiency. After the validation tests, the developed simulation model showed relatively high prediction accuracy when compared with the experimental results. The developed simulation model was then used to study the effects of equivalence ratio, biomass composition, moisture content as well as cogasification of sewage sludge and some findings are summarized as follows:

- Equivalence ratio highly influences the CGE value and the optimum equivalence ratio which gives the maximum CGE value was found to be 0.386.
- Feedstock with higher moisture content results in the lower CGE. This is mainly due to the decreasing of temperature inside the gasifier caused by the presence of moisture promotes the production of noncombustible products such as CO_2 through water-gas shift reaction.
- Adding sewage sludge in the feedstock results in the lower CGE, regardless of the equivalence ratio. This result was achieved on a Dry Ash Free basis, as the model is unable to consider the effects of ash clinkering and slagging that usually besets high ash content biomass such as sewage sludge.

Acknowledgments

This research programme is funded by the National Research Foundation (NRF), Prime Minister's Office, Singapore under its Campus for Research Excellence and Technological Enterprise (CREATE) programme. Grant Number R-706-001-101–281, National University of Singapore. The authors acknowledge the technical support of Xiuwu Jiang and Ye Shen on the project.

Notation

Q_{ext} = heat-transfer rate between the particle and its surrounding atmosphere, W
σ = Stephan Boltzmann constant
ε = particle emissivity
r = particle radius, m
h_T = convection heat-transfer coefficient, W/m^2/K
T_∞ = temperature of surroundings, K
T_p = temperature of particle, K
T_{react} = temperature of reactor, K
Q_{dry} = heat-transfer rate from drying process, W
H_p = particle enthalpy, J
m_W = mass of water, kg
m_s = mass of solid, kg
C_{psl} = heat capacity of solid matrix, J/kg/K
C_{pw}^{liq} = heat capacity of liquid water, J/kg/K
ρ_w^{vap} = water mass concentration at the surface of the particle in non-saturated conditions, kg/m
a_W = water activity
$F_{m,W}^{free,T}$ = mass flow rate of free water extracted from the particle at temperature Tp or Tevap, kg/s
$F_{m,W}^{bound,T}$ = mass flow rate of bound water extracted from the particle at temperature Tp or Tevap, Kg/s
k_m = mass-transfer coefficient, m/s
ρ_w^{sat} = water mass concentration in saturation, kg/m
Q_{react} = flow rate of heat due to reaction, W
ΔH_m^{vap} = enthalpy change of water vaporization, J/kg
ΔH_m^{des} = enthalpy change of water desorption, J/kg
C_{DB} = concentration of dried biomass, mol/m^3
$C_{char\ 1}$ = concentration of char 1, mol/m^3
$C_{char\ 2}$ = concentration of char 2, mol/m^3
$C_{PG\ 1}$ = concentration of pyrolysis gas 1, mol/m^3
$C_{PG\ 2}$ = concentration of pyrolysis gas 2, mol/m^3
C_i = concentration of species, mol/m^3
A_i = pre-exponential factor for reaction i
E_i = activation energy for reaction i, J/mol/K
n_x = molar density of species x, mol/m^3
n = summation of n_x of all species
A = area of gasifier, m^2
v = superficial gas velocity, m/s
z = axial distance, m
R_X = rate of formation of species x, mol/m^3/s
c_x = molar heat capacity, J/mol/K
ΔH_i = reaction enthalpy for the species i, kJ/kg
r_i = rate of reaction i, mol/m^3/s
P = total pressure of all gaseous species, Pa
ρ_{gas} = density of gas, kg/m^3
ρ_{air} = density of air, kg/m^3
Φ = equivalence ratio
t = time in gasifier, s

Literature Cited

1. Hoeven MV. CO_2 Emissions from Fuel Combustion: Highlights. Paris: International Energy Agency, 2011.
2. Saidur R, Abdelaziz EA, Demirbas A, Hossain MS, Mekhilef S. A review on biomass as a fuel for boilers. *Renew Sustain Energy Rev*. 2011;15:2262–2289.
3. Alauddin ZABZ, Lahijani P, Mohammadi M, Mohamed AR. Gasification of lignocellulosic biomass in fluidized beds for renewable energy development: a review. *Renew Sustain Energy Rev*. 2010;14:2852–2862.
4. Bridgewater AV. Review of fast pyrolysis of biomass and produce upgrading. *Biomass Bioenergy*. 2012;38:68–94.

5. Berndes G, Hoogwijk M, Brokek R. The contribution of biomass in the future global energy supply: a review of 17 studies. *Biomass Bioenergy*. 2003;25:1–28.
6. Gomez-Barea A, Leckner B. Modeling of biomass gasification in fluidized bed. *Prog Energy Combust Sci*. 2010;36:444–509.
7. Blasi CD. Modeling chemical and physical processes of wood and biomass pyrolysis. *Prog Energy Combust Sci*. 2008;34:47–90.
8. Puig-Arnavat M, Bruno JC, Coronas A. Review and analysis of biomass gasification models. *Renew Sustain Energy Rev*. 2010;14:2841–2851.
9. Cui HP, Grace JR. Fluidziation of biomass particles: a review of experimental multiphase flow aspects. *Chem Eng Sci*. 2007;62:45–55.
10. Kapanen A, Vikman M, Rajasärkkä J, Virta M, Itävaara M. Biotests for environmental quality assessment of composted sewage sludge. *Waste Manag*. 2013;33:1451–1460.
11. Mills N, Pearce P, Farrow J, Thorpe RB, Kirkby NF. Environmental & economic life cycle assessment of current & future sewage sludge to energy technologies. *Waste Manag*. 2014;34:185–195.
12. Winkler M. Sewage sludge treatments. *Chem Ind*. 1993;7:217–223.
13. Murgia S, Vascellari M, Cau G. Comprehensive CFD model of an air-blown coal-fired updraft gasifier. *Fuel*. 2012;101:129–138.
14. Kaewluan S, Pipatmanomai S. Gasification of high moisture rubber woodchip with rubber waste in a bubbling fluidized bed. *Fuel Process Technol*. 2011;92:671–677.
15. Folgueras MB, Diaz MR, Xiberta J. Pyrolysis of blends of different types of sewage sludge with one bituminous coal. *Energy*. 2004;30: 1079–1091.
16. Peng LX, Wang YX, Lei ZH, Cheng G. Co-gasification of wet sewage sludge and forestry waste in situ steam agent. *Bioresour Technol*. 2012;114:698–702.
17. Seggiani M, Puccini M, Raggio G, Vitolo S. Effect of sewage sludge contact on gas quality and solid residues produced by cogasification in an updraft gasifier. *Waste Manag*. 2012;32:1826–1834.
18. Pinto F, Lopes H, Andre RN, Dias M, Gulyurtlu I, Cabrita I. Effect of experimental conditions on gas quality and solids produced by sewage sludge cogasification. 1. Sewage sludge mixed with coal. *Energy Fuel*. 2007;21:2737–2745.
19. Pinto F, Andre RN, Lopes H, Dias M, Gulyurtlu I, Cabrita I. Effect of experimental conditions on gas quality and solids produced by sewage sludge cogasification. 2. Sewage sludge mixed with biomass. *Energy Fuel*. 2008;22:2314–2325.
20. Tigabwa YA, Murni MA, Suzana Y, Abrar I, Zakir K. Mathematical and computational approaches for design of biomass gasification for hydrogen production: a review. *Renew Sustain Energy Rev*. 2012;16: 2304–2315.
21. Sharma AK. Equilibrium and kinetic modeling of char reduction reactions in a downdraft biomass gasifier: a comparison. *Sol Energy*. 2008;82:918–928.
22. Ningbo G, Aimin L. Modeling and simulation of combined pyrolysis and reduction zone for a downdraft biomass gasifier. *Energy Convers Manag*. 2008;49:3483–3490.
23. Giltrap DL, McKibbin R, Barnesa GRG. A steady state model of gas-char reactions in a downdraft biomass gasifier. *Sol Energy*. 2003;74:85–91.
24. Wang Y, Kinoshita CM. Kinetic model of biomass gasification. *Sol Energy*. 1993;51:19–25.
25. Babu BV, Sheth PN. Modeling and simulation of reduction zone of downdraft biomass gasifier: effect of char reactivity factor. *Energy Convers Manag*. 2006;47:2602–2611.
26. Channiwala SA, Parikh PP. A unified correlation for estimating HHV of solid liquid and gaseous fuels. *Fuel*. 2002;81:1051–1063.
27. Besma K, Frederic M, Jean V, Fethi Z. Incineration of a small particle of wet sewage sludge: a numerical comparison between two states of the surrounding atmosphere. *J Hazard Mater*. 2007;147: 871–882.
28. Koufopanos CA, Lucchesi A, Maschio G. Kinetic modelling of the pyrolysis of biomass and biomass components. *Can J Chem Eng*. 1989;67:75–84.
29. Kashiwagi T, Nambu H. Global kinetic constants for thermal oxidative degradation of a cellulosic paper. *Combust Flame*. 1992;88:345–368.
30. Groppi G, Tronconi E, Forzatti P, Berg M. Mathematical modeling of catalytic combustors fuelled by gasified biomasses. *Catal Today*. 2000;59:151–162.
31. Johann CW, Susanne W, Harald R. Thermal conversion of biomass: comprehensive reactor and particle modeling. *AIChE J*. 2002;48: 2398–2411.
32. Bridgewater AV. Renewable fuels and chemicals by thermal processing of biomass. *Chem Eng J*. 2003;91:87–102.
33. Dogru M, Howarth CR, Akay G, Keskinler B, Malik AA. Gasification of hazelnut shells in a downdraft gasifier. *Energy*. 2002;27:415–427.
34. Bonnie JM, Sanford G, Martin AR. Coefficients for Calculating Thermodynamic and Transport Properties of Individual Species. *NASA Technical Memorandum 4513*, 1993.
35. Gao N, Li J, Qi B, Li A, Duan Y, Wang Z. Thermal analysis and products distribution of dried sewage sludge pyrolysis. *J Anal Appl Pyrol*. 2014;105:43–48.
36. Magdziarz A, Werle S. Analysis of the combustion and pyrolysis of dried sewage sludge by TGA and MS. *Waste Manag*. 2014;34: 174–179.
37. Arena U. Process and technological aspects of municipal solid waste gasification. *A review*. *Waste Manag*. 2012;32:625–639.
38. Lv PM, Xiong ZH, Chang J, Wu CZ, Chen Y, Zhu JX. An experimental study on biomass air–steam gasification in a fluidized bed. *Bioresour Technol*. 2004;95:95–101.
39. Mahishi M, Goswami DY. Thermodynamic optimization of biomass gasifier for hydrogen production. *Int J Hydrogen Energy*. 2007;323: 831–840.
40. Xie LP, Li T, Gao JD, Fei XN, Wu X, Jiang YG. Effect of moisture content in sewage sludge on air gasification. *Fuel Chem Technol*. 2010;38(5):615–620.
41. Zhang BP, Xiong SJ, Xiao B, Yu DK, Jia XY. Mechanism of wet sewage sludge pyrolysis in a tubular furnace. *Int J Hydrogen Energy*. 2011;36:355–363.
42. Gai C, Dong YP. Experimental study on non-woody biomass gasification in a down draft gasifier. *Int J Hydrogen Energy*. 2012;37: 4935–4944.
43. Kim YD, Yang CW, Kim BJ, Kim KS, Lee JW, Moon JH, Yang W, Yu TU, Lee UD. Air-blown gasification of woody biomass in a bubbling fluidized bed gasifier. *Appl Energy*. 2013; 112:414–420.
44. Maneerung T, Kawi S, Wang CH. Biomass gasification bottom ash as a source of CaO catalyst for biodiesel production via transesterification of palm oil. *Energy Convers Manag*. 2015;92: 234–243.
45. Pratik NS, Babu BV. Experimental studies on producer gas generation from wood waste in a downdraft biomass gasifier. *Bioresour Technol*. 2009;100:3127–3133.

Manuscript received Nov. 4, 2014, and revision received Mar. 13, 2015.